International Journal of Security and Its Applications
Vol. 10, No. 9 (2016), pp.243-256
http://dx.doi.org/10.14257/ijsia.2016.10.9.23

Simulation and Analysis for Error from Satellite Capture Segment Anti-spoofing

Liu You-ming[1], Feng Qi[1] and LIiTing-jun[1]

[1]*Department of Electronic and Information Engineering, Naval Aeronautical University, Yantai 264001, China*
E-mail: 15615659977@163.com

Abstract

The anti deception technology of the capture section is put forward, which is based on the idea of three-dimensional space compression domain. In the first part, the acquisition range of the signal is strictly controlled and the difficulty of the attack is increased. Doppler frequency and code phase estimation error are the key factor to affect the performance of the technology. The smaller the estimation error is, the more accurate the position of the real signal can be accurately determined.

Keywords*: Anti cheat; 3D spatial compression; Signal; Capture stage; Error*

1. Introduction

In the satellite navigation receiver tracking, measurement and positioning, the satellite signal must be captured before the capture of each satellite, the first should find the accurate frequency and code delay of the satellite, the two error must be less than the carrier ring and the code loop [1]. The typical receiver acquisition circuit is shown below:

The receiver should first determine the currently visible satellite, namely the need to search in the pseudo one dimensional code; due to the Doppler effect caused by the relative motion of satellite and receiver in the direction of the connection between the two. The receiver crystal oscillation frequency and satellite factors, receiving signal frequency ratio is not generally equal to the nominal value and need to search in the frequency dimension; at the same time, due to satellite to receiver distance constantly changing, plus the receiver has clock error, the received signal code phase values also changed. Therefore, it is needed in the code phase of one-dimensional search [2]. Visible, the so-called capture is a 3-D search to determine can be captured by satellite and the real frequency and code phase, through the examination of the corroborator output power in which frequency and code phase reached maximum, if the maximum output power exceeds the signal capture threshold can be thought to correspond to the maximum power of the replica signal parameters value, which is the signal capture the current received signal parameters estimation.

2. Three Dimensional Space Compression Technology

2.1. Signal Capture and Scene Analysis

In order to make an effective 3D search, it requires to roughly determine the three-dimensional search range, the receiver shall be with the three satellite almanac and ephemeris, the position of the receiver and current GPS time information. According to the theoretical calculation and the range Doppler roughly + 10kHz, the number of chips is 1023 and search step size of the frequency below 500Hz with each frequency channel code search time of 1ms.

ISSN: 1738-9976 IJSIA

In the search process, the problem of signal detection, setting the detection threshold in the search process, if the relevant integral amplitude exceeds the detection threshold, the receiver will be transferred to confirm the state.

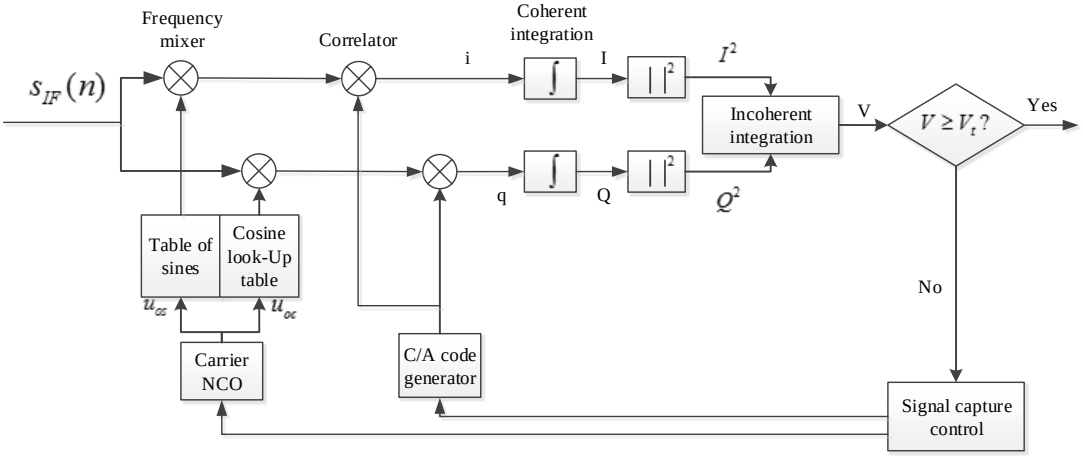

Figure 1. Signal Acquisition Circuit

The selection step of the capture threshold is to set up a false alarm rate P_{fa}, and to calculate the corresponding threshold value V_t according to the requirements of the false alarm rate. False alarm probability calculation formula is as follows:

$$P_{fa} = \int_{V_t}^{\infty} f_n(v)dv = \int_{V_t}^{\infty} \frac{v}{\sigma_n^2} e^{-\frac{v^2}{2\sigma_n^2}} dv = e^{-\frac{V_t^2}{2\sigma_n^2}} \tag{1}$$

On the formula, σ_n^2 the probability density function $f_n(v)$ when the signal is not present,the Rayleigh distribution is obtained as:

$$V_t = \sigma_n \sqrt{-2 \ln P_{fa}} \tag{2}$$

The most concern of the problem is to capture probability, sensitivity and capture rate. The capture probability is related to the selection V_t of the search area and the threshold P_d is:

$$P_d = \int_{V_t}^{\infty} f_s(v)dv = 1 - P_{md} \tag{3}$$

$f_n(v)$ The probability density function of the Rice distribution is the probability density function of the signal P_{md}. In order to improve the ability of the acquisition, the method of reducing the range of signal search and improving the signal to noise ratio of the received signal, the use of large parallel corroborator, the higher efficiency of the search algorithm, and so on.

Receivers capture strategy is usually ruled that the search domain maximum correlation peak for the satellite signal, when the receiver is at acquisition stage, spoofing of source can use power advantages make the target receiver to search for the deception related peak sentenced for real signals. The deception correlation peak signal

parameter extraction and transferred is to the track, thus the follow-up work will in the spoofing of source control development, so that we can be false localization results.

Foreign scholars put forward the use of monitoring signal to noise ratio or the absolute power of the method to counter this deception, due to the signal to noise ratio and absolute power of the measurement which can not be absolutely accurate, power in the receiver mobile or complex multi-path environment variables are many, practical limitations [3]. In addition, receiver remain power or signal to noise ratio of the area of vulnerability, source deceiving if it can be more flexible master the transmit power, the receiver receives the signal that will be more than the real satellite signals to the same and no more than typical power values. In this case, if the receiver does not take any anti spoofing, it still be deceived.

Assuming that the receiver is (10kHz, 1023), the receiver of the receiver is considered as the two case:

Scene one: in the target area it has been the existence of deception signal and real signal, the receiver boot, in the three-dimensional search area search satellite signal, carrying the implementation of signal capture;

Scene two: receiver of the target area already in normal tracking, implementation of deception to the target area implementation of suppressing interference, resulting in receiver loss of lock, then broadcast signal deception.

2.2. Anti Deception Technology

In the view of the scene one, considering the acquisition strategy to adjust the receiver to carry out the work: according to the experience threshold set a credible capture signal range, the range of the signal considered as abnormal signal, which will be excluded from the follow-up processing. The lower limit of the range that satellite signal capture threshold, and it set limit of the method which can be reference of the University of Calgary in Ali Jarfarnia *et al.* By evaluating the receiver receiving power of a real signal of typical value, it set up a typical threshold as the upper limit, if you enter the receiver signal which exceeds the upper limit, it is not real satellite signals in the follow-up processes to exclude, this technology can cannot antagonize the precise control of the receiving terminal receives the deception, low power.

Real signals and deception signals due to different power in the search area caused by the magnitude of the difference as shown below:

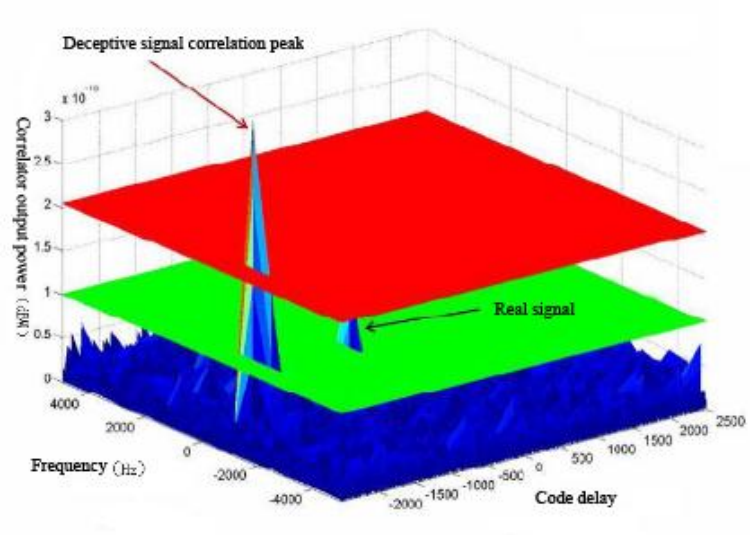

Figure 2. Schematic Diagram of Power Anti Fraud

If the receiver finds that two or more than two related peaks exceed the capture limit but not more than the upper bound, it is considered that the PRN signal of the satellite's representative is deceived. Although this technique can only detect the presence of a deception signal, it can not identify the correlation peak in the search area, but it can start the warning system to warn the user to be deceived and to take deception suppression or elimination in the follow-up process.

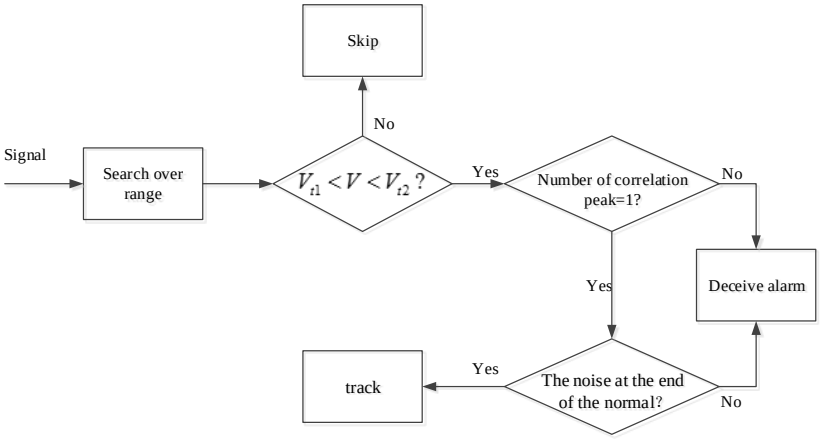

Figure 3. Scene One Anti Fraud Flow Chart

Pictured above, VT1 and Vt2 said lower and upper bounds on the range, if the signal is within the normal range, the need to judge correlation peak is more than one; with spoofing signal power, the increase in the number of may bottom noise uplift and real signals buried in noise floor below. Therefore, it is necessary to determine the noise floor is abnormal, if the background noise is higher than the typical value, you can start alarm mechanism.

For scenario two, the 3D spatial domain compression technique can be used to eliminate the deception signals other than the compressed domain. Assuming that the source can not be completely predicted by the receiver's position, velocity and acceleration, it is difficult to accurately match the three dimensional space position of the deception signal with the real signal. Due to receiver loss of lock in normal tracking state, from loss of lock before the satellite's pseudo code and loss of lock signal code phase and Doppler frequency shift, the receiver loss of lock before the loop parameters as the initial values, according to the satellite motion, movement of the receiver, receiver local clock punctual source accuracy and frequency drift rate of acquisition time code phase, Doppler estimated recapture the moments of the Doppler frequency and code phase. Because of the error, the calculation value is not accurate, and it can be determined by the calculation of the error of the Doppler frequency and code phase of the interval, plus the satellite pseudo code, that is a three-dimensional space compression, which is the basic idea of three-dimensional spatial domain compression technology.

The technology is suitable for the suppression of interference time is not long, if the target area has long been suppressed, the user will be judged by the attack, which lost the purpose of deception. At the same time, the receiver is the same as the first one, and it can be used to eliminate the problem.

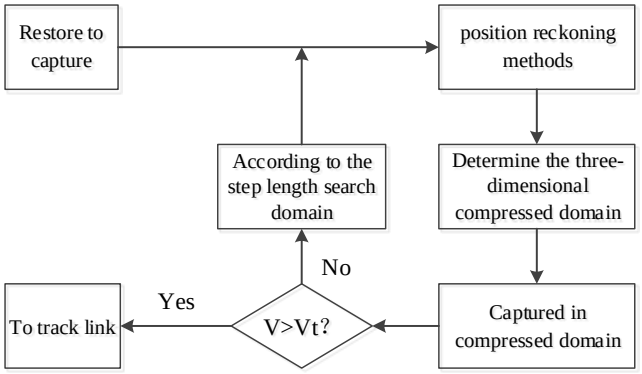

Figure 4. Two Scenario 4 Anti Fraud Flow Chart

The frequency and code phase of the Doppler frequency and code phase are described. The position of the satellite in the search area is known to be f_{10} n_{10}, after a period of time τ, to reach the new position Δn_{10}, $f_{10}+\Delta f_{10}$.

According to the position, velocity, acceleration and the drift of the receiver, Δf_{10} Δn_{10} the receiver can be divided into four scenarios: static, uniform speed, acceleration and acceleration.

- The receiver is in a static state

At this point, $v_R = 0$ the speed of the satellite motion can be considered as the same as the

$$\Delta f_{10} = \frac{\vec{v}_s \cdot \vec{l}}{\lambda \cdot \left|\vec{l}\right|} \tag{4}$$

$$\Delta n_{10} = \left(\tau \cdot \frac{f_{c10} + \Delta f_{c10}}{f_s} + n_{10} \right) (\mathrm{mod}\, n_T) \tag{5}$$

Among them, Δf_{10} recapturing unlocked during the Doppler shift distance, Δn_{10} to recapture moments of the number of chips, $\vec{v}_s$ satellite relative to a geocentric radial velocity, $\vec{l}$ receiver satellite connection vector, λ is for the satellite signal wavelength, f_{c10} the pseudo code frequency 1.023 MHz, Δf_{c10} code Doppler frequency, is the clock frequency of the receiver, for loss of lock time number of chips, code period the number of chips n_T, for C / A code n_T =1023. The Doppler frequency of the stationary state is caused only by the satellite velocity, and the offset is caused by the relative position.

- The receiver is in a state of uniform motion

At this point,keeping v_s firm, $v_R \neq 0$ if the relative satellite motion is assumed, then the correction (6) (7) two is as follows:

$$\Delta f_{10}{}' = \frac{(\vec{v}_s - \vec{v}_R) \cdot \vec{l}}{\lambda \cdot \left|\vec{l}\right|} \tag{6}$$

$$\Delta n_{10}' = \left(\tau \cdot \frac{f_{c10} + \Delta f'_{c10}}{f_s} + n_{10} \right) (\mathrm{mod}\, n_T) \tag{7}$$

At this point, $\Delta f'_{c10}$ the projection of the velocity vector at the receiver satellite connection is caused by the projection of the velocity vector of the user's velocity vector and the satellite velocity vector.

- The receiver in a uniformly accelerated motion

If the receiver acceleration is $\vec{a}_0$, the other variables are set to the same as the first two cases, then the correction (8) (9) two is as follows:

$$\Delta f_{10}'' = \frac{(\vec{v}_s + \vec{a}_0 \cdot \tau - \vec{v}_R) \cdot \vec{l}}{\lambda \cdot |\vec{l}|} \tag{8}$$

$$\Delta n_{10}'' = \left(\tau \cdot \frac{f_{c10} + \Delta f''_{c10}}{f_s} + n_{10} \right) (\mathrm{mod}\, n_T) \tag{9}$$

And similar to the above, $\Delta f''_{c10}$ is the synthetic speed of the code Doppler, relevant velocity are $\vec{v}_R \ \vec{v}_s \ \vec{a}_0 \cdot \tau$ which is projected on the receiver and satellite line.

- The receiver is in the acceleration state

At this point, assuming the receiver acceleration is $a(t)$, Doppler and the code piece position calculation formula is as follows:

$$\Delta f_{10}''' = \frac{(\vec{v}_s + \int_0^{\tau} t \cdot a(t) dt - \vec{v}_R) \cdot \vec{l}}{\lambda \cdot |\vec{l}|} \tag{10}$$

$$\Delta n_{10}''' = \left(\tau \cdot \frac{f_{c10} + \Delta f'''_{c10}}{f_s} + n_{10} \right) (\mathrm{mod}\, n_T) \tag{11}$$

In this scenario, $\Delta f'''_{c10}$ the rate of synthesis is caused by the code Doppler, the meaning of the synthetic speed reference to the aforementioned scene understanding.

According to the four kinds of life most common motion state and established the calculating model of receiver Doppler frequency as well as code phase, according to the model can get new 3D position, due to the presence of velocity error, position error, timing error (τ) and the receiver's internal clock frequency drift, according to the model to calculate the 3D position is not accurate, subsequent parts will calculate of error were analyzed. (simulation of the process to get the basis for the subsequent part of the variance)

3. Error Analysis

3.1. Doppler Frequency Estimation Error Analysis

Recapture time receiver Doppler frequency variation theoretical models:

$$f_{1\_r} = f_{0\_r} + \tau \dot{f}_{0\_r} + \frac{1}{2}\tau^2 \ddot{f}_{0\_r} + O(\cdot) \tag{12}$$

Where, f_{1_r} is for the re-acquisition time real value f_{0_r} for unlock the true value of time, τ from the loss of lock to interference experienced before re-acquisition clock count, $\dot{f}_{0\_r}$ the acceleration caused by the Doppler rate of change of the true value for the jerk caused by Doppler Le rate of change of acceleration rate of real value, $\ddot{f}_{0\_r}$ can be modeled as zero mean and variance of the Gaussian noise ${\sigma_{f_3}}^2$, $O(\cdot)$ higher order infinitesimal.

Recapture time receiver Doppler frequency measurements Model:

$$f_{1\_e} = (f_{0\_r} + n_{f_{0\_m}}) + \tau(\dot{f}_{0\_r} + n_{\dot{f}_{0\_m}}) + O(\cdot) \tag{13}$$

Where, f_{1_e} for the re-acquisition time estimates Doppler frequency measurement during Doppler frequency deviation $n_{f_{0\_m}}$ is out of lock, modeled as zero mean and variance of the Gaussian noise ${\sigma_{f_1}}^2$, for the period unlock the Doppler frequency change rate measurements offset, modeled as a zero mean and variance of the Gaussian noise ${\sigma_{f_2}}^2$.

Recapture time receiver Doppler measurement error models:

$$\Delta f = f_{1\_e} - f_{1\_r} = n_{f_{0\_m}} + \tau n_{\dot{f}_{0\_m}} - \frac{1}{2}\tau^2 \ddot{f}_{0\_r} + O(\cdot) \tag{14}$$

By the previously defined, it's clear that $n_{f_{0\_m}}$ $n_{\dot{f}_{0\_m}}$ $\ddot{f}_{0\_r}$ are independent, obeying the Doppler measurement errors are distributed:

$$\Delta f \sim N(0, \sigma_{f_1}^2 + \tau^2\sigma_{f_2}^2 + \frac{\tau^4}{4}\sigma_{f_3}^2) \tag{15}$$

3.2. Yards Phase Estimation error Analysis

Theoretical model of phase change of receiver code for heavy phase capture:

$$c_{1\_r} = c_{0\_r} + \tau\dot{c}_{0\_r} + \frac{1}{2}\cdot\tau^2\ddot{c}_{0\_r} + \frac{1}{6}\cdot\tau^3\dddot{c}_{0\_r} + O(\cdot) \tag{16}$$

Among them, c_{1_r} for the time code phase recapture the true value for the loss of lock time code phase true value c_{0_r} for the period unlock code Doppler real value, for

the period unlock code Doppler velocity actual value $\&_{0\_r}$, $\&\&_{0\_r}$ for the period unlock code large Doppler acceleration speed true value.

Recapture time receiver code phase change measurement model:

$$c_{1\_e} = (c_{0\_r} + n_{c_{0\_m}}) + (\&_{0\_m} + n_{\&_{0\_m}}) + \frac{1}{2}\tau^2(\&\&_{0\_r} + n_{\&\&_{0\_m}}) + O(\cdot) \tag{17}$$

Among them, c_{1_e} for the re-acquisition time code phase estimates, $n_{c_{0\_m}}$ -loss of lock time code phase measurement deviation can be modeled as a zero mean and variance of the Gaussian noise σ_c^2, $n_{\&_{0\_m}}$ for the period unlock code Doppler offset measurement period for the loss of lock code Doppler velocity measurement deviation $n_{\&\&_{0\_m}}$.

Recapture time receiver error code phase change model:

$$\Delta c = c_{1\_e} - c_{1\_r} = n_{c_{0\_m}} + \tau n_{\&_{0\_m}} + \frac{\tau^2}{2} n_{\&\&_{0\_m}} - \frac{\tau^3}{6} n_{\&\&\&_{0\_m}} + O(\cdot) \tag{18}$$

Satellite navigation signals provided radio frequencies $f_R = (1.023\times 10e6)\cdot l$, the Doppler frequency and code phase of the relationship, it was found, $n_{\&_{0\_m}} = \frac{n_{f_{0\_m}}}{l}$, $n_{\&\&_{0\_m}} = \frac{n_{\&_{f0\_m}}}{l}$ $n_{\&\&\&_{0\_m}} = \frac{n_{\&\&_{f0\_r}}}{l}$ thus formula () can be rewritten as:

$$\Delta c = n_{c_{0\_m}} + \frac{\tau}{l} n_{f_{0\_m}} + \frac{\tau^2}{2l} n_{\&_{f0\_m}} - \frac{\tau^3}{6l} n_{\&\&_{f0\_r}} + O(\cdot) \tag{19}$$

Because, $n_{c_{0\_m}}$, $n_{f_{0\_m}}$, $n_{\&_{f0\_m}}$ $\&\&_{0\_r}$ are independent, it was found to obey the following distribution:

$$\Delta c \sim N(0, \sigma_c^2 + \frac{\tau^2}{l^2}\sigma_{f_1}^2 + \frac{\tau^4}{4l^2}\sigma_{f_2}^2 + \frac{\tau^6}{36l^2}\sigma_{f_3}^2) \tag{20}$$

Asking too true signal appears on a compressed domain of probability, it needs to be two-dimensional probability density function $f(\Delta f, \Delta c)$, we can see and observe relevant, it shows:

$$f(\Delta f, \Delta c) = \frac{1}{2\pi\sigma_{\Delta f}\sigma_{\Delta c}\sqrt{1-\rho^2}} \exp\left[\frac{-1}{2(1-\rho^2)}\left(\frac{\Delta f^2}{\sigma_{\Delta f}^2} - 2\rho_{\Delta f \Delta c}\frac{\Delta f \Delta c}{\sigma_{\Delta f}\sigma_{\Delta c}} + \frac{\Delta c^2}{\sigma_{\Delta c}^2}\right)\right] \tag{21}$$

among which,

$$\rho_{\Delta f \Delta c} = \frac{\frac{\tau}{l}\sigma_{f_1}^2 + \frac{\tau^3}{2l}\sigma_{f_2}^2 + \frac{\tau^5}{12l}\sigma_{f_3}^2}{\sqrt{\sigma_{f_1}^2 + \tau^2\sigma_{f_2}^2 + \frac{\tau^4}{4}\sigma_{f_3}^2}\sqrt{\sigma_c^2 + \frac{\tau^2}{l^2}\sigma_{f_1}^2 + \frac{\tau^4}{4l^2}\sigma_{f_2}^2 + \frac{\tau^6}{36l^2}\sigma_{f_3}^2}}$$

Is Cross Correlation Coefficient

$$\left(\rho_{\Delta f \Delta c} = \frac{\operatorname{cov}(\Delta f, \Delta c)}{\sqrt{D(\Delta f)}\sqrt{D(\Delta c)}} = \frac{E(\Delta f \cdot \Delta c) - E(\Delta f) \cdot E(\Delta c)}{\sqrt{D(\Delta f)}\sqrt{D(\Delta c)}} \right) \tag{22}$$

In the compressed domain $f(\Delta f, \Delta c)$, the value of the value is the probability of a real signal falling on the interval, which is defined as the detection probability P, and the product of the probability of the receiver is the capture probability of the compressed domain.

$$P = \iint_{D_0} f(\Delta f, \Delta c) d\Delta f d\Delta c \tag{23}$$

If the signal is assumed to be uniformly distributed in the original search area, the probability density function is the probability density function $g(x, y)$.

$$g(x, y) = \frac{1}{20 \times 10e3 \times 1023} \tag{24}$$

In the compressed domain $g(x, y)$, the integration is the success rate, in other words, the specified interval can be defensive in the interval of the deception signal, we can know the probability of anti cheat

$$P\_spoof = 1 - \iint_{D_0} \frac{1}{2046 \times 10e4} d\Delta f d\Delta c \tag{25}$$

3.3. Data Simulation

According to the definition, it can be considered that σ_{f_1} the range of 1-3Hz, σ_{f_2} 0.05-0.2Hz/s, σ_{f_3} the range of 0.05-0.3, σ_c the range of 0.02-0.05 chip, the suppression time is desirable for arbitrary values between 0-10s, L1 GPS band to do reference, then l=1540.

(1) given σ_{f_1} =3, σ_{f_2} =0.2, σ_{f_3} =0.3, σ_c =0.03, the time0-10s, 20Hz*1 is the compression region, the relationship between the variance of the Doppler frequency and the phase of the code and the loss of the lock time is shown in the following diagram:

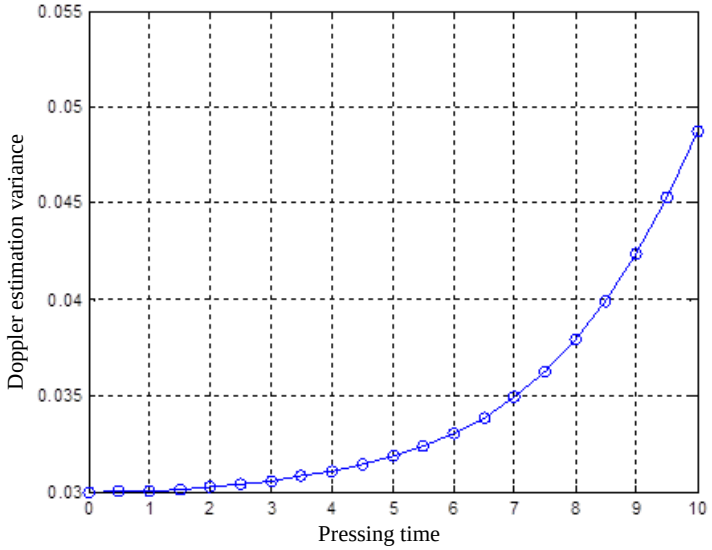

Figure 5. $\Delta f - \tau$ **Diagram**

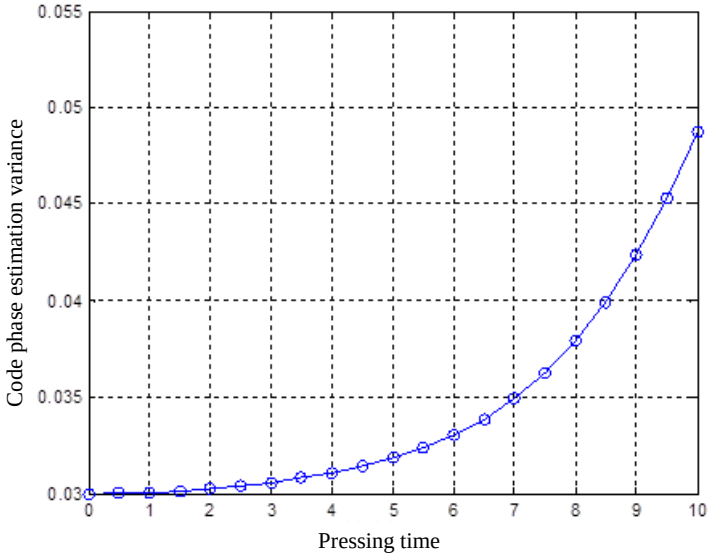

Figure 6. $\Delta c - \tau$ **Relation Graph**

(2) Given $\sigma_{f_1} = 3$, $\sigma_{f_2} = 0.2$, $\sigma_{f_3} = 0.3$, $\sigma_c = 0.03$, pressing time t = 5s, compression zone take 1 chip × (2-50) Hz, the actual integration region take ellipse, S_d represents an area of compression, P represents the probability of detection, P_spoof shows that anti-spoofing probability. Select the area of compression available and can capture probability and anti-spoofing probability of relationship:

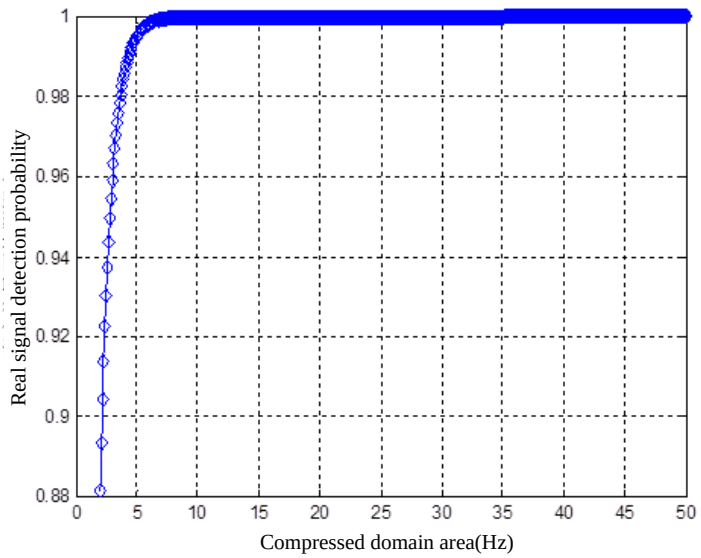

Figure 7. S_d -p Diagram

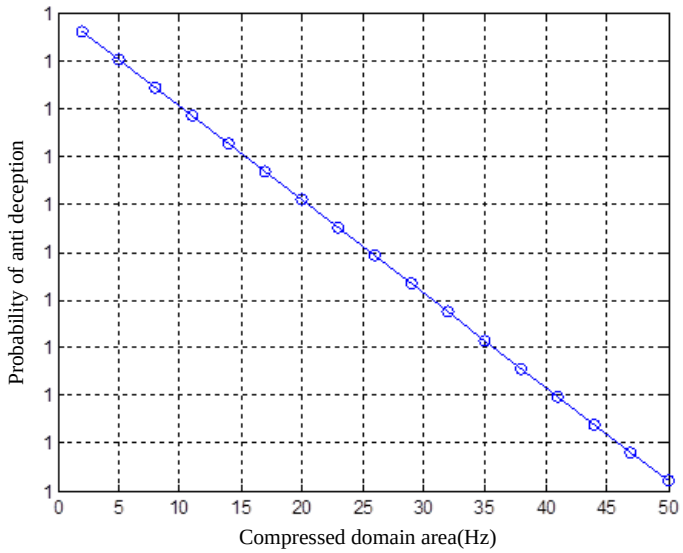

Figure 8. S_d - P_spoof Diagra

(3) given the pressing time t = 2 s, take 1 x 20 hz compression area, the actual take elliptic integral area, Doppler frequency estimation variance and code phase estimation variance increasing in accordance with the law, which can be under fixed compression area variance and relationship of the real signal detection probability:

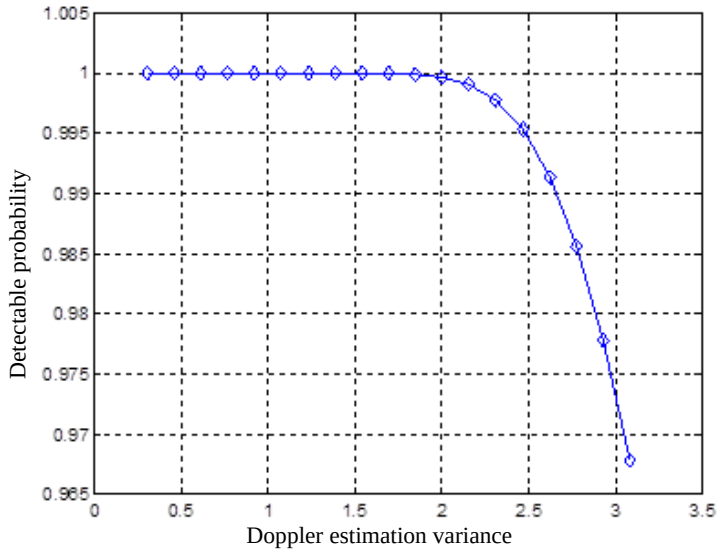

Figure 9. S_d -p Diagram

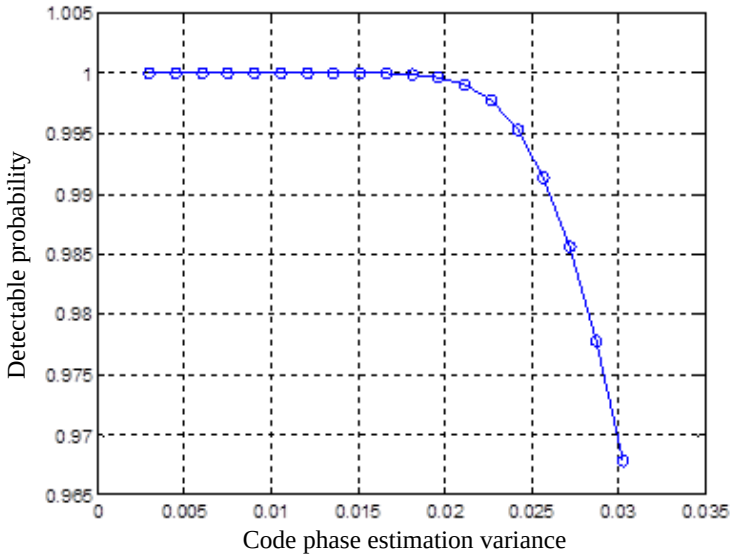

Figure 10. S_d - P_spoof Diagram

In real scenes, source of deceiving is impossible to occur without any deception, which is to estimate the deception and receiver relative distance and velocity and is used to suppress the interference by sliding the code phase of single fixed target or area all the receiver to cheat and bully cheat range bound than that the global search is much smaller. Assumed to deceive the source of a city all the receiver to cheat, namely area within a 10km * 10km cheat, pressing time is 3S, spoofing of source of distance resolution is set to 100 m, on the velocity resolution set of 10m / s, acceleration resolution is set to 2, which is still in the GPS L1 frequency segment, for example, cheating source code phase estimation error is 0.34 chip, Doppler frequency estimation error for 52.5Hz and Doppler changing rate estimation error for 10.5Hz/s, in view of the urban area, if user motion state is not too complicated, Doppler acceleration estimation error is set to 0.

4. Conclusion

Based on the three-dimensional space compression domain anti cheating technology analysis, it is concluded that: (1) when the pressing interference time t is firm, if the impact of Doppler frequency and code phase is related to the measurement error, $n_{c_{0\_m}}$ $n_{f_{0\_m}}$ $n_{\&_{f0\_m}}$ $\&_{0\_r}$ increase code phase and Doppler frequency estimation error and Δf Δc increase; when the effect of Doppler frequency and code phase measurement is error, certainly suppress interference time t increases, Doppler frequency and code phase estimation error increase. (2) in the three dimensional space compression domain, the detection probability and the anti cheat requirement of real signal are a pair of contradictory relations, increasing the range of the compressed domain can improve the detection probability and the risk of the receiver which is also increased. (3) Doppler frequency and code phase estimation error Δf Δc are the key factor to affect the performance of the technology. The smaller the estimation error is, the more accurate the position of the real signal can be accurately determined.

References

[1] Yang J., He S. and Lin Y., "Multimedia cloud transmission and storage system based on internet of things[J]", Multimedia Tools and Applications, **(2015)**, pp. 1-16.
[2] Lv Z., Yin T. and Han Y., "WebVR——web virtual reality engine based on P2P network[J]", Journal of Networks, vol. 6, no. 7, **(2011)**, pp. 990-998.
[3] Yang J., He S. and Lin Y., "Multimedia cloud transmission and storage system based on internet of things[J]", Multimedia Tools and Applications, **(2015)**.
[4] Guo C., Liu X. and Jin M., "The research on optimization of auto supply chain network robust model under macroeconomic fluctuations[J]", Chaos, Solitons & Fractals, **(2015)**.
[5] Li X., Lv Z. and Hu J., "XEarth: A 3D GIS Platform for managing massive city information[C]", //Computational Intelligence and Virtual Environments for Measurement Systems and Applications (CIVEMSA), 2015 IEEE International Conference on. IEEE, **(2015)**, pp. 1-6.
[6] Yang J., Chen B. and Zhou J., "A Low-Power and Portable Biomedical Device for Respiratory Monitoring with a Stable Power Source[J]", Sensors, vol. 15, no. 8, **(2015)**, pp. 19618-19632.
[7] G. Bao, L. Mi, Y. Geng and K. Pahlavan, "A computer vision based speed estimation technique for localiz ing the wireless capsule endoscope inside small intestine", 36th Annual International Conference of the IEEE Engineering in Medicine and Biology Society (EMBC), **(2014)** Aug.
[8] X. Song and Y. Geng, "Distributed community detection optimization algorithm for complex networks", Journal of Networks, vol. 9, no. 10, **(2014)** Jan., pp. 2758-2765.
[9] Jiang D., Ying X. and Han Y., "Collaborative multi-hop routing in cognitive wireless networks[J]", Wireless Personal Communications, **(2015)**, pp. 1-23.
[10] J. Hu and Z. Gao, "Modules identification in gene positive networks of hepatocellular carcinoma using Pearson agglomerative method and Pearson cohesion coupling modularity[J]", Journal of Applied Mathematics, 2012 **(2012)**.
[11] Jiang D., Xu Z. and Chen Z., "Joint time-frequency sparse estimation of large-scale network traffic[J]", Computer Networks, vol. 55, no. 15, **(2011)**, pp. 3533-3547. J. Hu, Z. Gao and W. Pan, "Multiangle Social Network Recommendation Algorithms and Similarity Network Evaluation[J]", Journal of Applied Mathematics, 2013 **(2013)**.
[12] M. Zhou, G. Bao, Y. Geng, B. Alkandari and X. Li, "Polyp detection and radius measurement in small intestine using video capsule endoscopy", 2014 7th International Conference on Biomedical Engineering and Informatics (BMEI), **(2014)** Oct.
[13] G. Yan, Y. Lv, Q. Wang and Y. Geng, "Routing algorithm based on delay rate in wireless cognitive radio network", Journal of Networks, vol. 9, no. 4, **(2014)** Jan., pp. 948-955.
[14] Lin Y., Yang J. and Lv Z., "A Self-Assessment Stereo Capture Model Applicable to the Internet of Things[J]", Sensors, vol. 15, no. 8, **(2015)**, pp. 20925-20944.
[15] Wang K., Zhou X. and Li T. "Optimizing load balancing and data-locality with data-aware scheduling[C]", Big Data (Big Data), 2014 IEEE International Conference on. IEEE, **(2014)**, pp. 119-128.
[16] Zhang L., He B. and Sun J., "Double Image Multi-Encryption Algorithm Based on Fractional Chaotic Time Series[J]", Journal of Computational and Theoretical Nanoscience, vol. 12, **(2015)**, pp. 1-7.

[17] Su T., Lv Z. and Gao S., "3d seabed: 3d modeling and visualization platform for the seabed[C]", Multimedia and Expo Workshops (ICMEW), 2014 IEEE International Conference on. IEEE, **(2014)**, pp. 1-6.
[18] Y. Geng, J. Chen, R. Fu, G. Bao and K. Pahlavan, "Enlighten wearable physiological monitoring systems: On-body rf characteristics based human motion classification using a support vector machine", IEEE transactions on mobile computing, vol. 1, no. 1, **(2015)** Apr., pp. 1-15.
[19] Lv Z., Halawani A. and Feng S., "Multimodal hand and foot gesture interaction for handheld devices[J]", ACM Transactions on Multimedia Computing, Communications, and Applications (TOMM), vol. 11, no. 1s, **(2015)**, p. 10.
[20] G. Liu, Y. Geng and K. Pahlavan, "Effects of calibration RFID tags on performance of inertial navigation in indoor environment", 2015 International Conference on Computing, Networking and Communications (ICNC), **(2015)** Feb.
[21] J. He, Y. Geng, Y. Wan, S. Li and K. Pahlavan, "A cyber physical test-bed for virtualization of RF access environment for body sensor network", IEEE Sensor Journal, vol. 13, no. 10, **(2013)** Oct., pp. 3826-3836,
[22] W. Huang and Y. Geng, "Identification Method of Attack Path Based on Immune Intrusion Detection, Journal of Networks", vol. 9, no. 4, **(2014)** Jan., pp. 964-971.
[23] Li X., Lv Z. and Hu J., "XEarth: A 3D GIS Platform for managing massive city information[C]", Computational Intelligence and Virtual Environments for Measurement Systems and Applications (CIVEMSA), 2015 IEEE International Conference on. IEEE, **(2015)**, pp. 1-6.
[24] J. He, Y. Geng, F. Liu and C. Xu, "CC-KF: Enhanced TOA Performance in Multipath and NLOS Indoor Extreme Environment", IEEE Sensor Journal, vol. 14, no. 11, **(2014)** Nov., pp. 3766-3774.
[25] N. Lu, C. Lu, Z. Yang and Y. Geng, "Modeling Framework for Mining Lifecycle Management", Journal of Networks, vol. 9, no. 3, **(2014)** Jan., pp. 719-725.

Authors

Liu You-ming, enrolled in Naval Aeronautical University, in communications and information engineering research, participated in a number of major national projects and Natural Science Foundation research projects, scientific research on communication has a great interest has published many articles in communication.

